(PDEs), additionally complicated by boundary conditions (BCs) at a moving boundary whose PDE itself involves the unknown velocity fields—is too difficult even for the most powerful modern computers. Fortunately, for certain domains in the space of parameters, simplified approximate descriptions are possible. In the most favorable cases, such a description would hinge on a *single* PDE, governing the evolution of some unknown quantity of the film—the quantity being the film *thickness* in all examples known to us. In the next section, we sketch such a theory for an *inclined* film; it leads to a dissipative-dispersive PDE for the film thickness. We argue that it is the most general leading-order equation of this kind which can be systematically derived from the full NS problem by using only well-controlled approximations (however, non-leading dissipative terms can be important when dispersion is large—as in [13, 29]). As a result, one simultaneously obtains the conditions for the theory to give a good approximation to the exact dynamics. We introduce the notion of *local-validity* conditions. These involve the characteristic *lengthscale* and *amplitude* of the current deviation of the surface from its average, Nusselt's position. Those characteristic quantities can *change* with time, and the local conditions can break down as a result. In such a case, the evolution equation (EE) based theory provides a good approximation for only a *limited* interval of time. We argue that such is the case for the Benney equation widely used to describe large-amplitude waves on inclined films (and that in fact no EE can do a better job). It is better, of course, if an approximation is good uniformly for all time. For this, certain *global-validity* conditions should be satisfied which, naturally, involve only time-independent, *basic* parameters—such as the Reynolds number, Weber number, etc. We obtain the most general theory of this type involving an evolution equation for film thickness. Where it is valid, it leads to *small-amplitude* waves, in accordance with the above remarks. The approach we use to obtain the outlined theory—which includes the evolution PDE, explicit expressions for velocities and pressure in terms of the PDE solutions, and the local- and global-validity conditions—is a further development of the *multiparametric* perturbation (MP) approach which has been suggested and used in our earlier papers [13, 14, 16, 19].

In section 3 we report some preliminary results of numerical simulations of our dissipative-dispersive evolution PDE. They have revealed unusual, highly-ordered but nonperiodic patterns on attractors of large-dispersion systems. For small dispersion, we observe qualitative agreement with transient patterns discovered in physical experiments [40]. This is somewhat surprising because their values of basic parameters are outside of the domain of validity of our theory (although comparatively close to it).

Summary and some conclusions are presented in the last section.

2 Theory hinged on a film thickness evolution equation

In this section we sketch a perturbation theory which includes an evolution PDE for film thickness, explicit expressions for velocities and pressures in terms of the film thickness, and conditions of validity for such a convenient approximation of the true evolution of the film. More complete derivations will be published elsewhere [24].

2.1 Large-amplitude waves and local-validity conditions

Consider a layer (of an average thickness $\overline{h}_0$; the overbar here and below indicates a *dimensional* quantity) of an incompressible Newtonian liquid of a density $\overline{\rho}$, viscosity $\overline{\mu}$, and surface tension $\overline{\sigma}$ flowing under the action of gravity (whose acceleration is $\overline{g}$) down an inclined solid plane whose angle with the horizontal is θ. Nusselt's velocity $\bar{U}$ at the interface

is $\bar{U} = \bar{g}\bar{h}_0^2 sin\theta/(2\bar{\nu})$ (where $\bar{\nu} = \overline{\mu}/\ \overline{\rho}$ is the kinematic viscosity). We nondimensionalize all quantities with units based on $\overline{\rho}$, $\overline{h}_0$, and $\bar{U}$. Then only three independent dimensionless *system parameters* appear in the dimensionless equations and boundary conditions; e.g. the angle θ, the Reynolds number $R = \bar{h}_0\bar{U}/\bar{\nu}$, and the Weber number $W = \sigma R/2$. The x axis of our system of coordinates is normal to the solid plane and directed away from it (and into the film); the y axis is in a spanwise direction; and the z axis is directed streamwise. The x, y, and z components of velocity are denoted, respectively, u, v, and w.

Let w_0 be the Nusselt velocity for an imaginary film of *constant* thickness h which is equal to the local thickness $h(y,z,t)$ of the real film (which is in line with experiments [1]): $w_0 = 2hx - x^2$. Similarly, the locally Nusselt pressure p_0 is by definition $p_0 = 2(h-x)\cot\theta/R$. [Note that w_0 and p_0 depend on y, z, and t (through $h(y,z,t)$) as well as on x.] The reference normal component of velocity u_0 is chosen to satisfy incompressibility, i.e., it is defined as the solution of $u_{0x} = -w_{0z}$ (the subscripts x, y, z, and t denote the corresponding partial derivatives), with the no-slip boundary condition $u_0 = 0$ at $x = 0$, which solution clearly is $u_0 = -x^2 h_z$. Finally, our spanwise reference velocity is identically equal to zero. The NS problem (see Appendix A) becomes an exact one for a new set of unknowns—h, u_1, v, w_1, and p_1—by the substitution $u = u_0 + u_1$, $w = w_0 + w_1$, and $p = p_0 + p_1$ (the remaining unknown v is not changed). For example, the kinematic boundary condition [Eq. (23) in Appendix A ($V = 0$)] at the free surface $x = h$ becomes

$$h_t + vh_y + (w_0 + w_1)h_z - u_0 - u_1 = 0. \tag{1}$$

Actually, analyzing derivations of known EEs, it is easy to see that these evolution equations always come from such a kinematic condition. Namely, the NS equations are simplified by discarding some terms, to become essentially *ordinary* differential equations (ODEs) for velocities and pressure as functions of x [with other independent variables entering as parameters only, through $h(y,z,t)$]. Having solved these simple (but nonhomogeneous) ODEs with constant coefficients, one substitutes those solutions for velocities in terms of h into the kinematic condition. This yields a closed PDE for h, the evolution equation. In our derivation, we follow this prescription as well, but we take care to discard only those terms in the NS equations which must be dropped if one is to obtain the *solvable* ODEs. In this way, one first finds p_1 from the x-NS equation, with the BC coming from the normal-stress balance condition at the free surface (for simplicity, the pressure of the ambient gas is neglected). Clearly, in this problem for p_1, all terms containing one or more of the unknowns u_1, v, and w_1 need to be discarded. Next, the y-NS equation is recast into an ODE for v. Here, only terms containing u_1 or/and w_1 must be discarded; the p_1-term is retained as it is now a known expression in terms of h. However, all terms containing v, except for the viscous one with v_{xx}, are to be discarded as well—otherwise we will not have a solvable ODE in x. It turns out that this requirement automatically eliminates all terms with u_1 and w_1 as well. If we denote by A the characteristic amplitude of the surface deviation $\eta \equiv h - 1$, and let T, Y, and Z be, respectively, the characteristic time-, $y-$, and $z-$scales, then, for example, the condition that the *neglected* viscous terms be smaller than the ones retained, after estimating these quantities in terms of the characteristic scales, yields the requirement $(1+A)^2/L^2 \ll 1$ [where by definition $L = \min(Y,Z)$]. Thus, as a consequence of our "derivability" principle, we have obtained the small-slope condition—which usually is rather *postulated* in the "lubrication" or "long-wave" derivations. In obtaining this condition, we have used the estimates of the derivatives: For example, for the x-derivatives, we have $\partial/\partial x \sim 1/(1+A)$, in the sense that $\partial/\partial x \sim 1$ if $A \sim 1$ or $A \ll 1$, and $\partial/\partial x \sim 1/A$ if $A \gg 1$ (since $h \sim A$ for $A \gg 1$ and the velocities change from being zero at $x = 0$ to

their full magnitudes at $x = h$; hence, the characteristic lengthscale of change is h, which is $\sim A$). Also, $\partial/\partial t \sim 1/T$, $\partial^2/\partial y^2 \sim 1/Y^2$, $\partial^2/\partial y \partial z \sim 1/YZ$, etc. Similar to the small slope condition above, $(R/T)(1+A)^2 \ll 1$ follows; etc. In fact, one can estimate the velocities even before solving the equations; for example, one finds

$$v \sim \max\left[\frac{(1+A)^3 A}{ZY},\ \frac{WA(1+A)^2}{YZ^2},\ \frac{WA(1+A)^2}{Y^3},\ \frac{\cot\theta A(1+A)^2}{Y}\right].$$

Substituting such estimates into inequalities demanding the smallness of terms which must be discarded, one finally arrives at the set of independent conditions for the derivation to be justified. These validity conditions can be combined as follows:

$$\max\left[\frac{(1+A)W}{L^3}, \frac{(1+A)\cot\theta}{L}, \frac{(1+A)^4 R}{L}, \frac{(1+A)^2}{L^2}\right] \ll 1, \tag{2}$$

where we have assumed, for simplicity, that either $Y \sim Z$ or $Y \gg Z$—which so far has been the case in all experiments. [All these conditions can be obtained e.g. already from the requirement of negligibility of the term containing u_{1z} in BC for w_1, Eq. (20) in Appendix A.] Due to these conditions, even some terms which can be retained in the equations—and handled, in principle, without any problem—are shown to be actually negligible; some other terms are estimated to lead to a negligible contribution into the final evolution equation and therefore can be discarded as well. As a result, one can see that the expression for p_1 is in fact the solution of the problem [see Eq. (14) and (21) of Appendix A]

$$p_{1x} = [u_{0xx}/R =] - 2h_z/R,$$

$$p_1 = \left[2u_{0x}/R - \sigma\nabla^2 h =\right] - 4hh_z/R - \sigma\nabla^2 h \qquad (x = h),$$

that is

$$p_1 = -2(x+h)h_z/R - \sigma\nabla^2 h \tag{3}$$

(here $\nabla^2 = \partial^2/\partial y^2 + \partial^2/\partial z^2$). Note that this pressure contains a *viscous* contribution in addition to the usual surface-tension part (and the reference pressure p_0 is of a purely hydrostatic origin).

The equation for v is, in the simplified form, $(1/R)v_{xx} = p_{0y} + p_{1y}$. The boundary conditions are $v = 0$ at $x = 0$ and, from a tangential-stress balance [see Eq. (19) in Appendix A], $v_x = -u_{0y} + w_{0y}h_z - 2u_{0x}h_y$ at $x = h$. The solution of this problem for v is the expression in terms of h given by Eq. (24) in Appendix B. The equation for w_1 is the (simplified) z-NS equation:

$$w_{1xx} = Ru_0 w_{0x} + w_0 R w_{0z} - 2Rw_{0z} + R(p_{0z} + p_{1z}) - w_{0yy} - w_{0zz} + Rw_{0t}.$$

(Note that we use the system of coordinates of a moving reference frame, whose ($z-$)velocity with respect to the solid plane is $V = 2$—that is the same as the well-known phase velocity of the infinitesimal waves. Velocities however are those measured in the *laboratory* frame.) We also have the boundary conditions $w_1 = 0$ at $x = 0$ and, from a tangential-stress balance equation [see Eq. (20) in Appendix A] at $x = h$, $w_{1x} = -u_{0z} - 2u_{0x}h_z + w_{0y}h_y + 2w_{0z}h_z$. The solution is Eq. (25) of Appendix B. Next, the equation for u_1 comes from the continuity equation: $u_{1x} = -v_y - w_{1z}$, where v and w_1 are already known [see (24) and (25) in Appendix B]; and the no-slip BC requires that $u_1 = 0$ at $x = 0$. The solution is Eq. (26)

in Appendix B. Substituting the expressions (24), (25), and (26) for velocities in terms of h (taken at $x = h$) into the kinematic condition (1), we arrive at the EE

$$h_t - \frac{R}{12}(h^5)_{tz} + 2(h^2-1)h_z + R\left[\frac{5}{6}h^4h_z - \frac{3}{10}h^6h_z\right]_z \tag{4}$$

$$-\frac{2}{3}\nabla\cdot\left[h^3(\cot\theta - W\nabla^2)\nabla h\right] + 2h^4\nabla^2 h_z = 0.$$

(A *one-dimensional* version of this equation—which also lacked the last, odd-derivative term—appeared before, e.g. in [33]. Also, we have omitted other dispersive terms which are negligible in the limit of small amplitudes, see Eq. (5) below.) The solutions of this equation give a good approximation to the true evolution of the thickness h—for some time, at least—as long as the conditions (2) are satisfied.

Using those conditions along with the estimates of all the members of the EE (4) in terms of the current amplitude A, the (current) lengthscale L, and the basic parameters, it is easy to see that if A is *not* small, the equation is written as simply $h_t + 2(h^2-1)h_z = 0$ (or just $h_t + 2h^2h_z = 0$ in the laboratory reference frame): all other terms of the EE (4) turn out to be much smaller than the remaining two. The solutions of the last equation are well known to exhibit steepening of the wavefronts up to a breakdown in a finite time. It follows that the EE (4) cannot be valid globally, i.e. for all time. But this EE is in fact equivalent to the (widely used) Benney equation: The latter follows from the former (in the laboratory reference frame and with the dispersion term omitted) if one substitutes the expression $-2h^2h_z$ instead of h_t (the "trade of time- for space-derivative" of [2]) in the second term of (4). Thus, the Benney equation can approximate the large-amplitude waves *at best* for a finite time—a fact that was discussed in detail in [17]. As in the latter paper, we again arrive at the conclusion that a film thickness EE which would provide a good time-uniform approximation to large-amplitude waves (on films flowing down inclined planes) *does not exist* (whereas for films flowing down *cylinders* such an equation was given in [16]).

The two equations, (4) and Benney one, are however not obliged to be equivalent when the conditions (2) break down, and there are indications that our equation has a chance to avoid the explosive solutions (see e.g. [26, 43, 44]) which mar the Benney equation: Indeed, it is the term with the highest power of h (in fact, h^6) in its coefficient which causes the explosion in the Benney equation, but our h^6-term enters with the *opposite* sign. Thus, although neither of the two equations is capable of a *quantitatively* good description of the large-time behavior, the EE (4) might be a better choice to be used as a *qualitative* model for large-amplitude waves. This possibility makes the equation worthwhile of a further investigation (which we have not attempted as yet).

2.2 General evolution PDE, global-validity conditions, and MP approach

At *small* amplitudes, writing $h = 1 + \eta$, (where $\eta \sim A \ll 1$), we arrive from the large-amplitude evolution equation (4) at the EE for small-amplitude waves:

$$\eta_t + 4\eta\eta_z + \frac{2}{3}\delta\eta_{zz} - \frac{2}{3}\cot\theta\,\eta_{yy} + \frac{2}{3}W\nabla^4\eta + 2\nabla^2\eta_z = 0, \tag{5}$$

where by definition $\delta \equiv (4R/5 - \cot\theta)$. The linear stability analysis (see below) shows that one needs $\delta > 0$—which condition we assume fulfilled from now on—to have an instability and thus the possibility of an interesting nonlinear behavior. It follows that

$R > (5/4)\cot\theta > \cot\theta$. We use this inequality together with $A \ll 1$ to transform the general conditions (2) and obtain the local-validity conditions for the small-amplitude EE (5):

$$\max\left(W/L^3,\ R/L,\ 1/L^2,\ A\right) \ll 1. \tag{6}$$

One can see from our derivation of the EE (5) that the third, destabilizing term originates from the inertia terms of the NS equations. The (stabilizing) fourth and fifth terms are due respectively to hydrostatic and capillary (i.e. surface-tension) parts of the pressure. Finally, the last, odd-derivative term is due to the viscous part of the pressure. This term is purely *dispersive:* it does not lead to either growth or decay of the amplitude of surface deviation η. Such a term also appeared in the EE obtained by Topper and Kawahara [49] for an almost vertical plane (naturally, the hydrostatic term was absent in that equation): they used the small angle of the plane with the vertical as their (single) perturbation parameter. Our derivation shows their assumption to be unnecessary: For *any* inclination θ (and any value of W), if R is close to $R_c \equiv 5\cot\theta/4$—so that δ is sufficiently small—then the equation (5) is valid, and its dispersive term is not small; simultaneously, the hydrostatic term can be large as well (but $Y \gg Z$). Without the dispersive term, the equation of Topper and Kawahara becomes the one obtained by Nepomnyashchy [42], whose one-dimensional version is the Kuramoto-Sivashinsky equation [35, 46]. All of these equations are thus limiting cases of our EE (5).

Due to the dissipativeness of the EE (5), the system evolves towards an attractor and thus essentially forgets its initial conditions. On the attractor, there can be fluctuations, but no systematic change in time. Then, following the ideas of our earlier papers [3, 19], the destabilizing inertia term should be of the same order of magnitude as the stabilizing, capillary one. Hence, the (dimensionless) characteristic lengthscale *at large times* L_a is estimated to be

$$L_a = (W/\delta)^{1/2}.$$

Similarly, the asymptotic magnitude of the characteristic amplitude A_a is determined by the balance between the nonlinear "convective" term and either the dispersive term or the capillary one (whichever is larger): $A_a = \max(W/L_a^3,\ 1/L_a^2)$. Using these estimates, the condition (6) can be written as $\max(W/L_a^3,\ R/L_a,\ 1/L_a^2) \ll 1$. Noting that $W/L_a^3 = \delta/L_a$ and $R = (5/4)(\delta + \cot\theta) > \delta$, we finally can write this as $\max\left(R/L_a,\ L_a^{-2}\right) \ll 1$. Thus the validity conditions are

$$\alpha \equiv 1/L_a^2 \ll 1 \quad \text{and} \quad \beta \equiv R/L_a \ll 1. \tag{7}$$

These conditions involve only the basic (time-independent) parameters of the flow. If the basic parameters satisfy these conditions, the EE (5) is valid (yields a good approximation) for all time. Hence, these conditions may be termed the *global-validity* conditions.

We can transform Eq. (5) to a "canonical " form–which would contain a minimum of "tunable" constants—by rescaling $\eta = N\widetilde{\eta}$, $z = L_a\widetilde{z}$, $y = L_a\widetilde{y}$, and $t = T_a\widetilde{t}$. We take $N = W/(6L^3)$ and $T_a = 3W/2\delta^2$. Dropping the tildes in the notations of variables, the resulting canonical form of the small-amplitude evolution equation is

$$\eta_t + \eta\eta_z + \eta_{zz} - \kappa\eta_{yy} + \nabla^4\eta + \lambda\nabla^2\eta_z = 0, \tag{8}$$

where $\kappa = \cot\theta/\delta$ and $\lambda = 3/\sqrt{W\delta}$.

For a small perturbation in the form of a normal mode, $\eta \propto \exp(st - i\omega t)\exp i(jy + kz)$, one readily finds—from the linearized version of Eq. (8)—the growth rate s: $s =$

$-\kappa\,(j)^2 - (j)^4 + \left[1 - 2\,(j)^2\right] k^2 - k^4$. The streamwise wavenumber k_{max} corresponding to the maximum growth rate (at fixed j) is obtained from $\partial s/\partial k^2 = 0$: it is $k_{max}^2 = 1/2 - j^2$. It follows that the maximum growth rate $s_{max}(\kappa; j)$ is

$$s_{max} = 1/4 - j^2(1+\kappa). \tag{9}$$

Thus, s_{max} is a linearly decreasing function of κ for every fixed j. While the scope of linear stability theory is limited, it is nevertheless helpful in interpreting some of the results of our numerical simulations of EE (8), as will be seen below.

The way we have derived the above theory is in fact a refinement of the less-formal version of the multiparametric perturbation approach used in [3, 13, 16, 19]. In the more formal version of the method (see [13, 14, 16]), one would represent the variables of the problem as multiple series in powers of two (or more in other physical problems) independent perturbation parameters, α and β of Eq. (7) (this is why we call the method *multiparametric).* Then the evolution equation and the expressions for velocities and pressure follow from the leading-order equations for the leading-order coefficients of the power series. There is no need for this more formal procedure unless one is concerned with higher-order corrections to the leading-order results.

We note that all the terms of Eq. (8) can be found among the about one hundred explicitly given terms of an equation obtained by Krishna and Lin [34], who used formal expansions in a long wave parameter (see also [45]). Our derivation thus establishes that only a small number of those terms should be included in the equation: All other terms are negligible whenever the equation can yield a good approximation, i.e. under conditions (7) or (6).

3 Numerical simulations of evolution PDE

Here we report some preliminary results of our simulations of the dissipative-dispersive equation (8) with periodic boundary conditions. We believe that the results can be insensitive to the exact form of the boundary conditions only when the dimensions of the domain are sufficiently large that it contains many "elementary structures" (for example, it is known that such simulations give "surprisingly good results" [23] for similar problems of the boundary-layer wave transitions). Hence, we solved Eq. (8) on extended spatial intervals, $0 \le y \le 2\pi p$ and $0 \le z \le 2\pi q$, where $p \gg 1$ and $q \gg 1$.

We used spatial grids of up to 256×256 nodes, with the Fourier pseudospectral method for spatial derivatives and with appropriate dealiasing. Time marching was done (in the Fourier space) by using Adams-Bashforth and/or Runge-Kutta methods. We checked the results by refining the space grids and time steps; by verifying the volume conservation, $\int \eta dydz = 0$; etc.

We have used a variety of initial conditions. Some of those were motivated by the experiments [40]: The inlet conditions of their experiments were modeled by our initial conditions [see Eq. (12) below].

In the remainder of this section, we discuss results of our numerical simulations, including (i) the effect of dispersion on the large-time behavior of the film surface near the attractor; (ii) an investigation of two-dimensional stationary waves and their stability; and (iii) the effect of varying the wavenumber of the initial "forcing" on the transient states, in comparison with the experiments of Liu *et al.* [40].

3.1 Large dispersion: Unusual 3-D patterns on attractors

The most striking result of our numerical simulations has been a discovery of highly nontrivial patterns in time-asymptotic states for the *strongly dispersive* cases of Eq. (8), $\lambda \gg 1$. These self-organized states are reached by the system starting from the small-amplitude (3-D) *white-noise* conditions (whereas with the same, random initial conditions we see no ordered patterns, but just chaos, in the large-time states of the surface in the case of *small* dispersion). Invariably, spatial patterns studied up to now in fluid-dynamical experiments—as well as in solid state physics, nonlinear optics, chemistry, and biology—were almost periodic, at least locally (see e.g. [9]). In contrast, our results reveal that patterns of quite a different character can exist on attractors of dissipative-dispersive systems. The patterns we report here consist of two *subpatterns* of localized surface deviations. One of these subpatterns is a V-shaped array of larger-amplitude *bulges* on the film surface. Those are surrounded by smaller-amplitude *droplets.* These constitute the second, lattice-like subpattern. Each of the two subpatterns spans the entire domain of the flow. However, the bulge formation moves as a whole "percolating" through the droplet subpattern (which itself moves as a whole with respect to the solid plate).

Figure 1 shows a snapshot of the film surface at $t = 3200$, for a film with $\lambda = 50$ (and $p = q = 16$) on a vertical wall (i.e., $\kappa = 0$). (There, because of the scaling, the small slopes are exaggerated.) Figure 2—which presents the evolution of "energy" $E \propto \int \eta^2 dydz$—testifies to the fact that by that time the system has approached its asymptotic state in which there is no further systematic change. Figures 3(a) and 3(b) show the above-mentioned two-stream nature of the pattern: The V-shaped formation (consisting of 13 large bulges; see also Fig. 1) moves as a whole with a certain velocity, and the small-amplitude background moves uniformly as well, but in the opposite direction (in appropriate reference frames); in addition, the droplet subpattern slowly changes in time. (An especially clear view of those motions is provided by our computer animations.) We note that one component of this spatiotemporal pattern, the bulges, have been already discovered in [48], for $\lambda = 25$ and $p = q = 64/(2\pi)$. (They simulated a dissipative-dispersive equation [49] in which the κ term of Eq. (8) was absent, since the derivation [49] was based on a certain—unnecessary, as we discussed above—assumption.) But apparently the authors of [48] used only contour plots as their graphics tools, and overlooked the second, droplet subpattern—and thus the entire complex, dynamical character of the two-phase pattern.

One can see in Figs. 2 and 3 the following features: The characteristic lengthscales for the both subpatterns are ~ 1. The same follows from the requirement [3, 19] that the destabilizing (third) term of Eq. (8) balances the stabilizing (fourth-order) one so that the amplitude may remain, on average, constant. However, the amplitude of a bulge *chaotically fluctuates*. The amplitude of these fluctuations is approximately equal to the amplitude of the droplets (~ 10). The amplitude of a large bulge (~ 100 here) is estimated to be $\sim \lambda$ from the balance between the dispersive and nonlinear terms of Eq. (8).

The V-shaped formation of bulges moves downstream with the velocity (in the moving reference frame) $\approx 4.5\beta\overline{U}$. The observed streamwise velocity of the other, small-amplitude subpattern is $\approx (2 - 8.0\beta)\overline{U}$ in the laboratory reference frame. So, this subpattern moves down the wall if $\beta < 1/4$, but *up* the wall otherwise. An order-of-magnitude estimate of the droplet velocity c can be obtained by balancing the term $c\eta_z$ (which will appear in Eq. (8) as a result of the transition to the co-moving reference frame) with the (large) dispersive term. Then the amplitude of droplets is estimated from the requirement that the nonlinear term be of the same order as the (small) dissipative terms. These estimates appear to be in agreement with what is observed in our numerical simulations. There is a perturbation

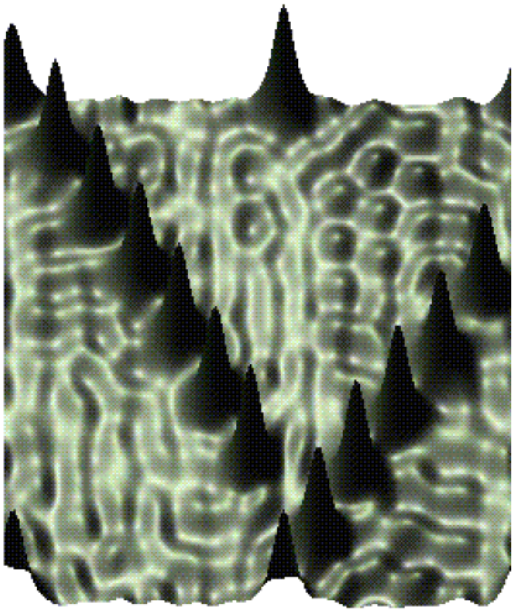

FIG. 1. *Snapshot of the pattern on an attractor of Eq. (8) with* $\kappa = 0$ *(i.e. the scaled surface of a film flowing down a vertical plate, here—down the page, with illumination from the top left),* $\lambda = 50$*, and periodic boundary conditions on* $0 < y, z \leq 32\pi$*: a view in an oblique direction, for* $t = 3200$.

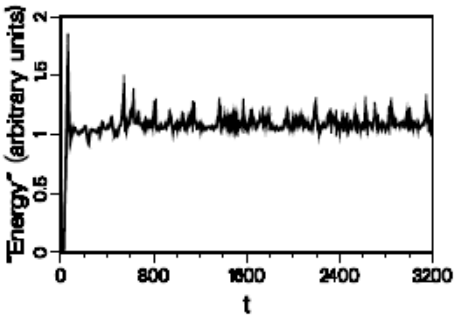

FIG. 2. *Evolution of the surface deviation "energy"* $\int \eta^2 dydz$ *from an initial small-amplitude "white-noise" surface to an attractor of Eq. (8). The snapshots of Figs. 1 and 3 were taken near the end of this run.*

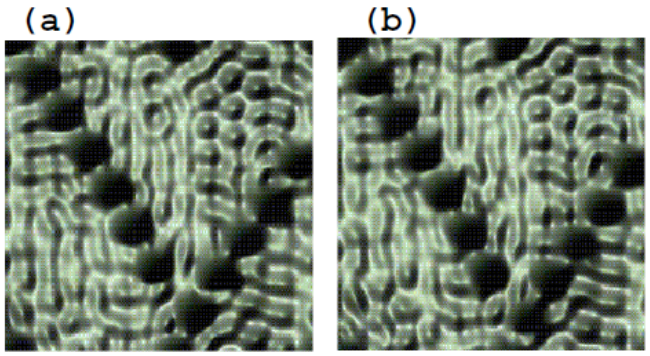

FIG. 3. *(a) Cross-stream view of the pattern shown in Fig. 1. (b) Same as in (a) but after a time interval* $\Delta t = 0.25$. *Note that the vertical motion of the V-shaped formation of bulges from (a) to (b) is in the opposite direction to that of the droplet pattern.*

theory of weak interactions (e.g. [4, 11, 30]) for the "pulses" [29] of the 1-D version of Eq. (8), similar to [22]. However, no analytic solution is available for a solitary 3-D bulge (we speak in such cases of 3-D structures because the underlying velocity field depends on all three spatial coordinates; see also [40]), and therefore the prospects for constructing a similar interaction theory for the 3-D bulges are limited.

Droplets collide with bulges. As a droplet runs into a bulge, the bulge's amplitude increases momentarily. Shortly after that, it decreases again while a droplet separates from the opposite side of the bulge. These interactions are (almost) reversible, like interactions of KdV pulses [51], and unlike the irreversible coalescences of 2-D pulses discovered in [20] and [32] for highly nonlinear dissipative equations.

As the value of λ for the above simulations is varied (from 0 to 50), the attractor pattern changes. At small λ, we observe chaotic (although 3-D) waveforms. [Note that at $\lambda = 0$, the 1-D version of Eq. (8) is the Kuramoto-Sivashinsky equation, which on extended spatial intervals yields *chaotic* attractors; see e.g. [9].] For larger λ however the ordering effect of dispersion becomes increasingly evident: The amplitude separation into the bulges and the background becomes noticeable for $\lambda \sim 5$, and continues to grow with λ.

In another set of simulations, with $\lambda = 50$ and $p = q = 16$, we vary κ from 0 to 50. For small values of κ (≤ 0.2), the attractor pattern is similar to that discussed above for $\kappa = 0$. As κ is increased however the film surface becomes more chaotic and the amplitude of droplets increases up to becoming comparable to that of the bulges. Starting from $\kappa \cong 50$, the overall pattern has just one phase: it consists of large-amplitude, roughly 2-D ripples elongated in the y direction. This finds some explanation in the linear theory: The formation of large-amplitude bulges requires that many spanwise (as well as streamwise) modes be present. However, as κ grows, modes with higher spanwise wavenumbers stabilize [see Eq. (9)], which suppresses the formation of 3-D bulges.

Similar to Eq. (8), we [12, 18] have derived an evolution equation for a film which flows down a vertical *cylinder*. The only essential difference between that equation and Eq. (8) is the opposite sign of the κ term. However, this term disappears in the case of a vertical planar film, which is also the limit of an infinitely large radius of the cylinder. Our simulations showed that even for $p = 5$ the corresponding κ term of the annular-film equation is sufficiently small so that the results essentially coincide with those of the $\kappa = 0$

version of Eq. (8). Thus, the theory leading to Eq. (8) can be checked in experiments with films flowing down vertical cylinders. The cylinder should be sufficiently long so that the waves could have time to approach the attractor. One finds that with $\widetilde{h_0} \sim 1$ mm, the radius ~ 1 cm, and with the conditions (7), in order for the cylinder to be not too long, the liquid should be sufficiently viscous, in fact several hundred times as viscous as water. This requirement can be easily satisfied with e.g. a glycerol-water solution. [We note that one can see a straight row of bulges in the photograph of a film flowing down a cylinder in Fig. 2 of Ref. [5]; however, the β-condition of validity (7) was not strictly satisfied there.]

Among other results, our simulations confirm that—as had been implicitly assumed in deriving the global-validity conditions for EE—the solutions of our equation remain bounded. Furthermore, the amplitude of the solution is of the same order of magnitude as the estimates obtained by pairwise balance of terms in the evolution equation.

These simulations also demonstrate that the large-time behavior of the solutions of (8) is essentially insensitive to the initial conditions: The solution evolves toward an attractor whose nature is dependent on the basic parameters of the system.

3.2 Small dispersion: 2-D stationary waves and their stability

During our numerical simulations with one- and two-frequency forcing, we have observed 2-D stationary waves which are stable to 3-D disturbances at certain wavenumbers of the primary forcing. For wavenumbers k between 0.5 and 1.0, these stationary waves consist mainly of the fundamental and a few of its stable overtones at smaller levels. Such stationary waves for different film evolution equations were constructed by many researchers (e.g. [10, 25, 41, 50]; it seems however that most of the huge number of such stationary solutions are very unstable, and only few of them are observed in experiments—only when artificial forcing is present at that). In the wavenumber range $0.5 < k < 1$, the stationary waves can be well approximated as two-mode equilibria consisting of the unstable fundamental and the stable overtone. In the absence of dispersion, approximating η as the Fourier series truncated at the Nth member,

$$\eta(z,t) = \sum_{n=1}^{N} A_n(t) e^{inkz} + c.c., \tag{10}$$

one obtains from Eq. (8), for $N = 2$, the Galerkin system $dA_1/dt = s_1 A_1 - ikA_1^* A_2$ and $dA_2/dt = s_2 A_2 - ikA_1 A_1$, where $s_n = n^2k^2(1 - n^2k^2)$. Hence, at a stationary state ($\partial A_n/\partial t = 0$), assuming A_1 to be real, one finds

$$A_1 = \sqrt{s_1|s_2|}/k; \quad A_2 = -is_1/k.$$

Our numerical simulations have indeed resulted in stationary waves with mode amplitudes and phase relations similar to that given by the above expressions.

Similarly, including the third harmonic, so that $\eta_0 = \sum_{n=1}^{3} A_n e^{inkz} + c.c.$, we find for the stationary wave

$$A_1^2 = \frac{s_2 X}{k^2\,[1 - 6X/s_3]}, \quad A_2 = ik\frac{A_1^2}{[s_2 + (6k^2/s_3)A_1^2]}, \quad A_3 = -\frac{3k^2}{s_3}\frac{A_1^3}{[s_2 + (6k^2/s_3)A_1^2]}$$

(in the reference frame where A_1 is positive), where $X = -s_3/6 + 1/6\sqrt{s_3^2 - 12 s_1 s_3}$. While the amplitude of the additional mode is small in comparison with that of A_1 and A_2, its

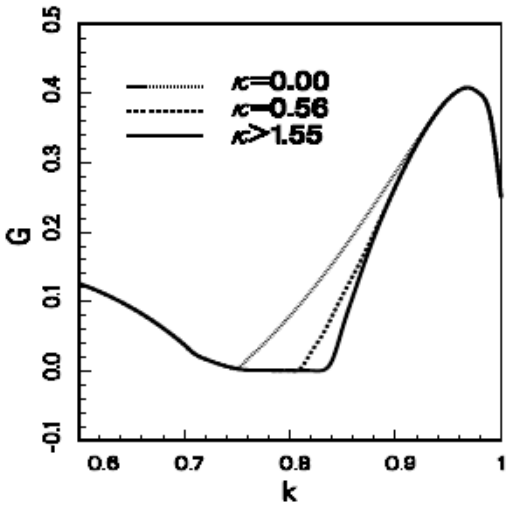

FIG. 4. *(a) Growth rate (for the values of κ shown in the legend) and (b) the streamwise Bloch's wavenumber of the fastest-growing Bloch's mode [see Eq. (11)] of the secondary instability for $\kappa = 0.56$ ($\lambda = 0.057$).*

inclusion makes the agreement with the numerically found stationary waves even more close. For a small disturbance which is a normal mode of the Bloch type (introduced a long time ago for the stationary wavefunctions of an electron in the periodic field of the crystal lattice; see e.g. [36]),

$$H \sim e^{Pt+ik(Jy+Kz)} \sum_{m=-l}^{l} B_m e^{imkz}, \tag{11}$$

one obtains, after substituting $\eta = \eta_0 + H$ into Eq. (8) and linearizing it, an eigenvalue problem for P. (This is the so-called Floquet analysis—which was applied to film waves in [8], and was used earlier in other hydrodynamic problems, see e.g. [23, 31]. We believe Bloch's rather than Floquet's name is more appropriate in this context; see e.g. [15, 21, 47]). The eigenvalues $P = P_r + iP_i$ were found by solving the eigenvalue problem numerically. The number of modes l in the Fourier series truncation (11) was increased until the eigenvalues converged within an acceptable accuracy. We are interested only in the eigenvalue whose real part is maximum. This maximum real part $G = \max P_r$—the growth rate of the instability—is shown as a function of the primary wavenumber k in Fig. 4(a), for three different values of the parameter κ. The corresponding value of the streamwise Bloch's wavenumber K at which the maximum growth occurs is shown in Fig. 4(b) for the intermediate value $\kappa = 0.56$ (which value corresponds to the parameters of some of the experiments of [40]). One sees from Fig. 4(a) that for the case of a vertical plane—as was already noted in numerical studies by Chang *et al.* [7]—there are no 2-D stationary waves *stable* to 3-D disturbances. However, we find that, as κ increases from 0, a window of wavenumbers appears over which 2-D stationary waves are stable to all disturbances, including the 3-D ones. The window reaches its maximum extent at

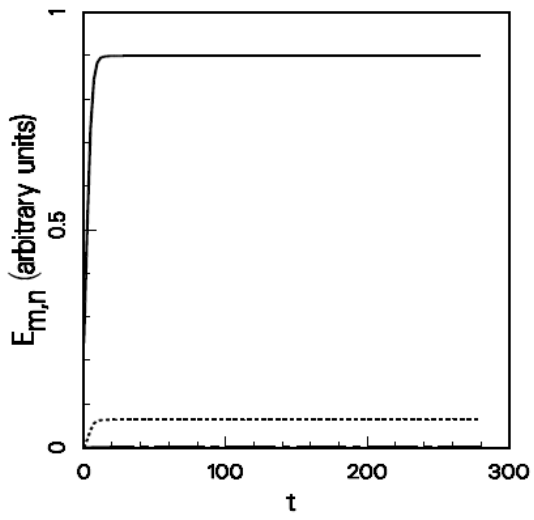

FIG. 5. *Evolution of the Fourier-mode energies of the surface deviation starting from the general forcing initial condition, Eq. (12) ($\kappa = 0.56, \lambda = 0.057; p = 8, q = 47$), and into a stationary-wave state. The only modes noticeable are the fundamental ($m = 0, n = 36$; the solid line) and its first overtone ($m = 0, n = 72$); other modes never reach an appreciable level of energy.*

$\kappa \approx 1.55$ and remains the same for all $\kappa > 1.55$, in which domain of κ the most unstable (or least stable) disturbances are two-dimensional. Since the κ term of our Eq. (8) vanishes for the streamwise disturbances, the curve in Fig. 4(a) characterizing the stability to *all* disturbances for $\kappa > 1.55$ coincides with the one which deals with only 2-D disturbances in the case of a vertical film, $\kappa = 0$, shown in Fig. 5 of Ref. [7].

Our numerical simulations have confirmed the existence of the island of stability. To obtain the stationary waves, we have used "one-frequency-forcing" initial conditions, i.e. those with one dominant *fundamental* Fourier mode (which was 2-D, streamwise). Its harmonics, the first oblique subharmonic, and noise were present at smaller levels. In Fig. 5 we show the evolution of the "energies" $E_{m,n}$ of the Fourier modes, defined as

$$E_{m,n} = \mid a_{mn} \mid^2$$

where a_{mn} is the Fourier coefficient:

$$\eta = \sum a_{mn} e^{i(my/p + nz/q)}.$$

In this simulation with $p = 8$ and $q = 47$, the initial condition was of the form

$$\begin{aligned}(12)\quad \eta(y,z;t=0) \;=\; & A_f \cos(n_f \tilde{z}) + A_h[\cos(2n_f\tilde{z} - \phi_1) + \cos(3n_f\tilde{z} - \phi_2)] \\ & + A_h[\cos(n_f\tilde{z} - \phi_3) + \cos(2n_f\tilde{z} - \phi_4) + \cos(3n_f\tilde{z} - \phi_5)]\cos\tilde{y} \\ & + A_{sub}[\cos(0.5n_f\tilde{z} - \phi_6) + \cos(0.5n_f\tilde{z} - \phi_7)\cos\tilde{y}] \\ & + \text{small white noise},\end{aligned}$$

with $A_f = 1.2$, $A_h = A_{sub} = 0.05$, $n_f = 36$; in (12), $\tilde{y} = y/p$, $\tilde{z} = z/q$, and ϕ_i are independently generated random phases. The only modes noticeable in Fig. 5 are the

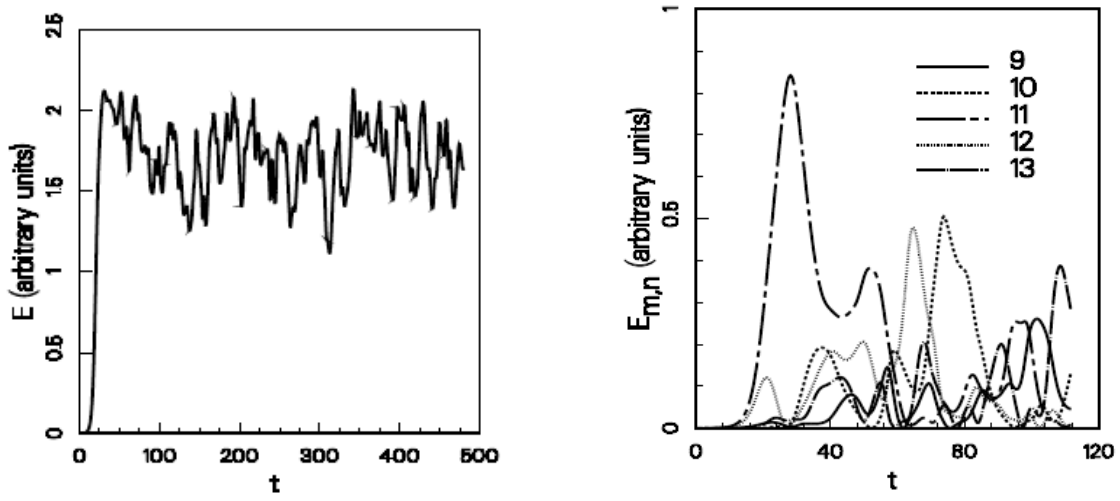

FIG. 6. *Evolution from a 2-D "white-noise" initial condition ($\kappa = \lambda = 0; q = 16$). (a) Total energy and (b) energies of the most active Fourier modes (the number shown in the legend next to each line is the corresponding value of n; note that the $n = 11$ mode is the fastest-growing one according to the linear theory).*

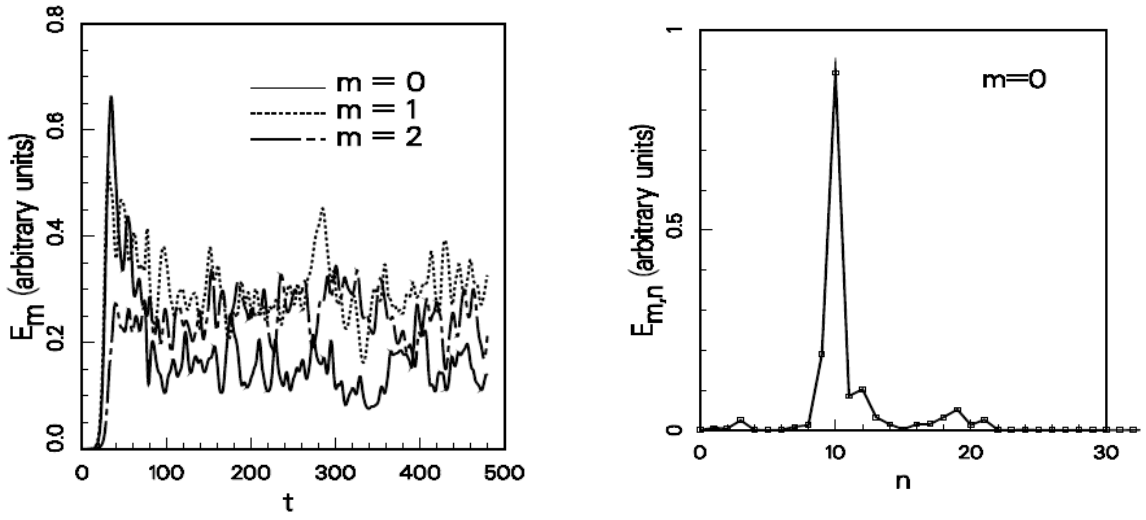

FIG. 7. *Evolution from a 3-D white-noise initial condition ($\kappa = 0.0, \lambda = 0.0; p = 8, q = 16$). (a) Evolution of combined energies $E_m \equiv \sum_n E_{m,n}$ for the three lowest values of m (indicated in the legend). (b) Energies E_{0n} of the streamwise ($m = 0$) Fourier modes for $t = 32$ (the solid line is a guide to the eye).*

fundamental ($m = 0, n = 36$) and its first overtone ($m = 0, n = 72$); other modes never develop. Also, we observed in our simulations that the addition of "white noise" into the initial condition does not prevent the system from attaining the stationary state, provided the signal (i.e. the amplitude of the primary forcing) is at least an order of magnitude larger than the noise.

For those wavenumbers not inside the stable window, it is still possible to obtain quasi-stationary waves, when the initial forcing contains only one frequency. We found that the "Floquet" growth rate depicted in figure 4(a) is capable of giving some estimate of the lifetimes of the quasiequilibria. However, this linear stability analysis is of limited use: It often fails to predict what patterns emerge as a result of instability, because the system quickly reaches a nonlinear stage which can bring to prominence modes other than those dominating the initial stage of instability.

Finally, our numerical simulations with the 2-D (Fig. 6) and 3-D (Fig. 7) "white-noise" initial condition never yielded any stationary (or even quasistationary) waves. After the stage of initial exponential growth [see Fig. 6(a)], near the maximum of the total "energy" $E = \sum_{m,n} E_{m,n}$ (which is proportional to the spatial average of η^2), the fastest-growing mode of the linear theory is definitely the one that is dominant [see Fig. 6(b)]. For some limited time (around $t \sim 65$) the maximum shifts to higher wavenumbers. The latter however still fall short of the stability window—in which this maximum should have ended according to the spirit of the interesting transition scenarios suggested in [6, 7, 8] (for a different model of film waves. On the experimental side, there seems to be little evidence that such a shortening of the characteristic wavelength does occur.) Gradually, as the total energy fluctuates considerably around its average level [see Fig. 6(a)], the energy spreads wider and wider over the spectrum of modes, while the film surface evolves from a quasi-sinusoidal state to a fully chaotic one.

3.3 Small dispersion: Transient patterns and physical experiments

While the large-time behavior of the film is insensitive to the initial conditions (see subsection 3.1), the transient states *are* dependent on the initial condition (unless the latter is a predominantly monochromatic forcing of type (12) with the fundamental wavenumber in the window of stability). For different initial conditions, the film surface exhibits a variety of patterns. Our study of the transient states has been primarily motivated by the recent experiments of Liu *et al.* [40]. They perturbed the flow at its inlet with sinusoidal pressure variations at a fixed frequency f. In addition to this single frequency "forcing", in some of their experiments, a secondary forcing at the subharmonic frequency $f/2$ was used. The amplitude of the secondary forcing was considerably smaller than that of the primary one. (The motivation for using the secondary forcing was to enhance any broad-band subharmonic resonances). We modelled this inlet forcing by the initial conditions of type (12), with $A_h \ll A_f$ and $A_{sub} \ll A_f$.

In addition to the initial conditions, we have also been motivated by the experiments of Liu *et al.* in the selection of values of the parameters κ and λ for our simulations. One can see that the values $\kappa = 0.56$ and $\lambda = 0.06$ we used in most cases are fairly typical of the experiments of Ref. [40]. We again point out that values of parameters (R, W, and θ) in those experiments lie outside the domain of validity of Eq. (8) [there exist however many other sets (R, W, θ) which lead to the same values of λ and κ, and at the same time do satisfy the validity conditions (7)].

When the wavenumber of primary forcing (k) is close to the neutral wavenumber, and in

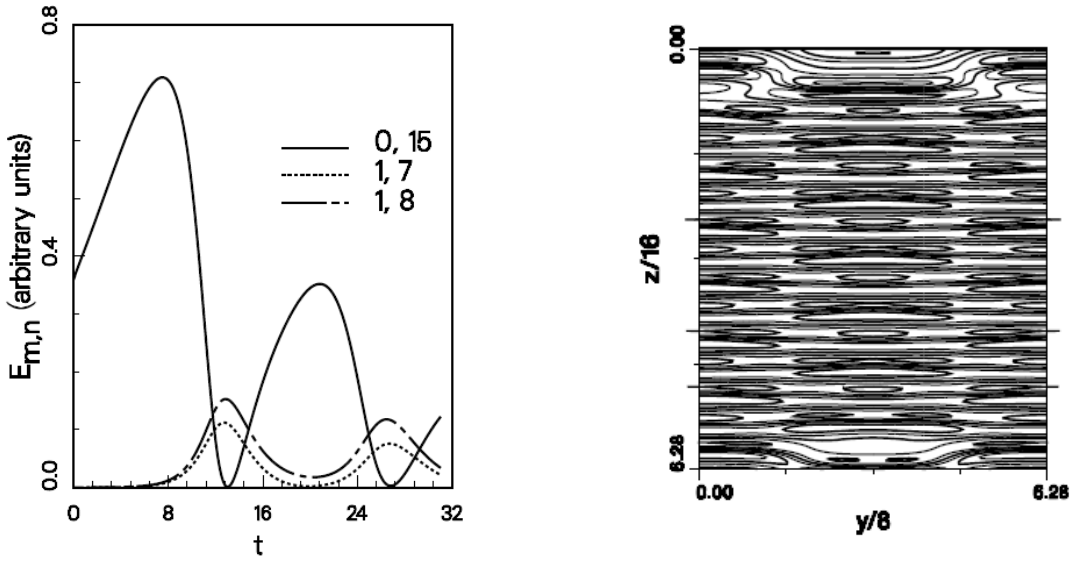

FIG. 8. *Subharmonic interaction of Fourier modes in a run with the initial condition (13) whose frequency of primary forcing is close to the neutral one ($q = 16, n_f = 15$). (a) Evolution of energies of the principal Fourier modes (the numbers shown in the legend next to each line are the corresponding values of m and n, in this order). Note that since n_f is an odd number, there are two "almost-subharmonic" modes, one with $n = 7$ and the other with $n = 8$. (b) Checkerboard pattern of the film surface for $t = 21$ (c.f. Fig. 12 of [40]). The interval between two neighboring isothickness contours is* 0.6.

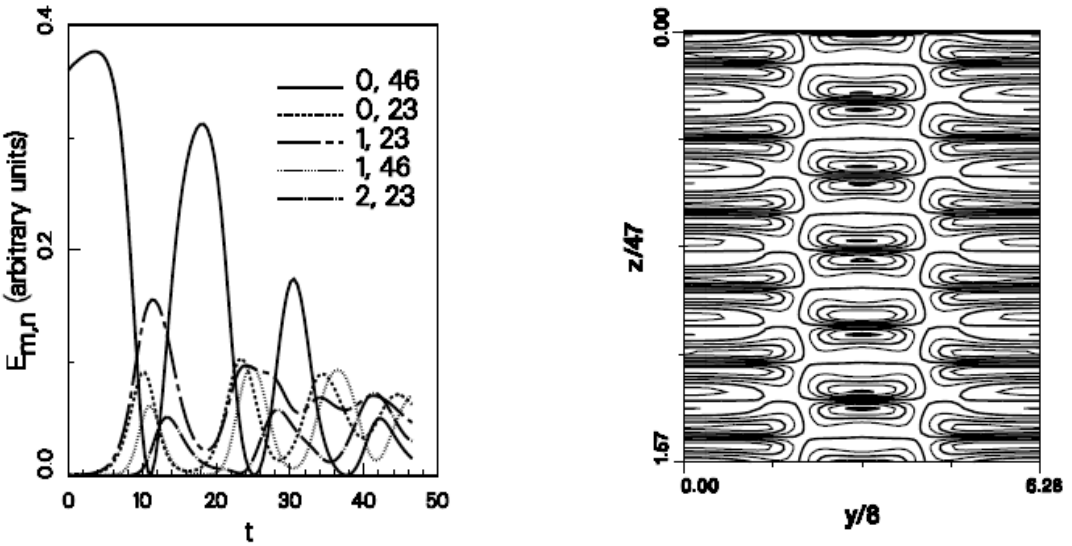

FIG. 9. *Similar to Fig. 8 but for a run starting from the general initial condition (12), with $q = 47$ and $n_f = 46$. Note that the checkerboard-like pattern in (b) is not perfect, but the streamwise period-doubling is clear ($t = 14.6$; only one quarter of the streamwise extent of the periodicity domain is shown; the interval between two neighboring isothickness contours is* 0.6).

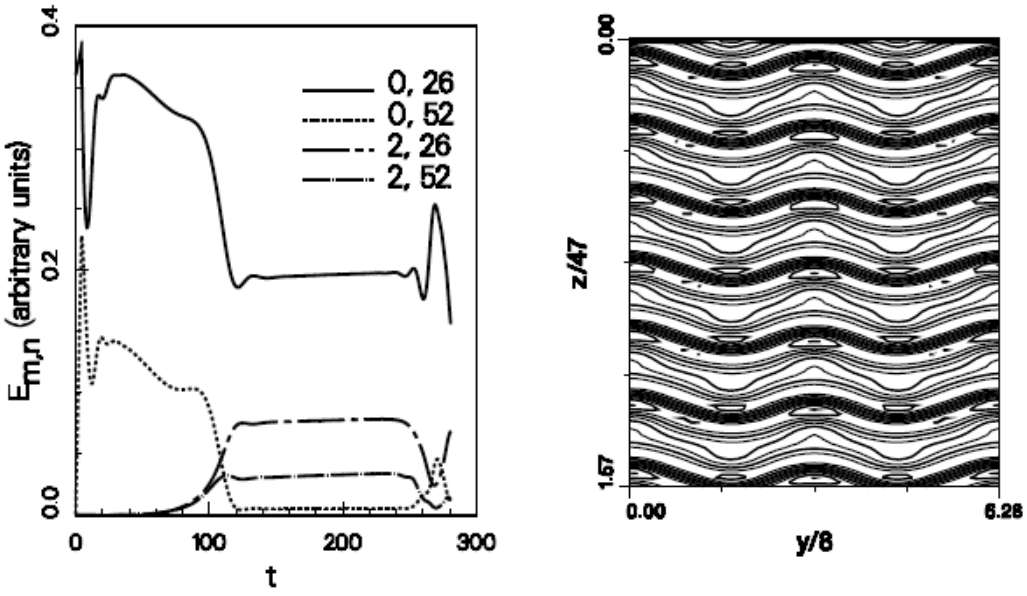

FIG. 10. *3-D "synchronous instability" of initially (almost) 2-D waves, Eq. (12) with* $A_{sub} = 0$, *at lower forcing frequencies* ($q = 47, n_f = 26$). *(a) Evolution of energies of four principal Fourier modes. Note the quasistaionary-wave state beginning at some time after* $t = 120$. *(b) The surface pattern at* $t = 164$ ($\kappa = 0.18, \lambda = 0.05$*: c.f. Fig. 1(a) of [40]). The interval between two neighboring isothickness contours is* 0.4.

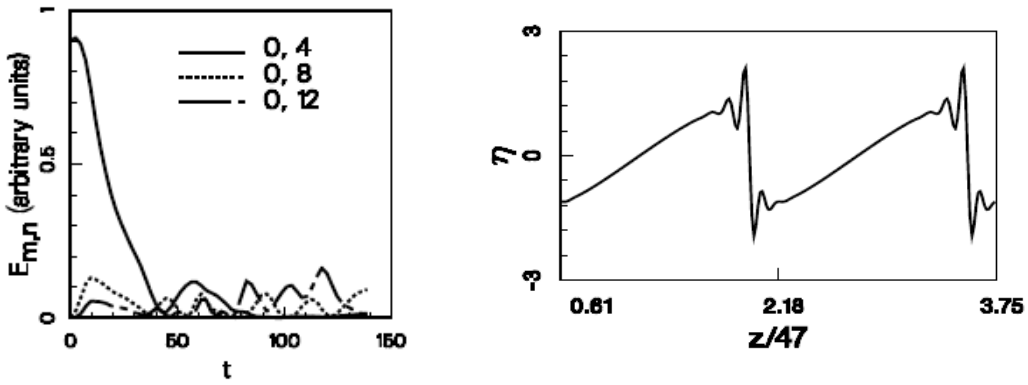

FIG. 11. *"Solitary wave" pattern in a run with a low-frequency forcing (the initial condition (12), with* $q = 47$ *and* $n_f = 4$; $\kappa = 0.56, \lambda = 0.057$). *(a) Evolution of energies of some principal Fourier modes (the numbers shown in the legend next to each line are the corresponding values of* m *and* n, *in that order). (b) The wave profile at* $t = 19.3$. *Only a part of the train of four solitary waves is shown (c.f. Fig. 2(b) of [40]).*

the presence of secondary forcing at the subharmonic frequency [i.e. $A_{sub} \neq 0$ in Eq. (12)], the oblique subharmonic interacts very strongly with the fundamental. This is illustrated in Fig. 8 for an idealized initial condition,

$$\eta(y, z; t = 0) = A_f \cos(n_f \tilde{z}) + A_{sub} \cos(0.5 n_f \tilde{z}) \cos \tilde{y} \tag{13}$$

with $A_f = 1.2$, $A_{sub} = 0.05$, and $n_f = 15$ (while $q = 16$). Figure 8(a) shows the strong interaction with the exchange of energy between the fundamental and the oblique (detuned) subharmonics. The surface exhibits checkerboard patterns such as the one in Fig. 8(b), which is seen to resemble the checkerboard pattern of "cat eyes" in Fig. 12 of Ref. [40]. With the full initial forcing (12) however other modes become significant, as is evident in Fig. 9(a), and while the period doubling is obvious, the chekerboard pattern in Fig. 9(b) is not perfect. Indeed, the characteristic property of the oblique subharmonic $\cos(n_f \tilde{z}/2 + \phi) \cos \tilde{y}$ which is responsible for the checkerboard structure, its invariance under the transformation $(\tilde{z}, \tilde{y}) \rightarrow (\tilde{z} + 2\pi/n_f,\ \tilde{y} + \pi)$, is readily seen to be not shared by such modes as the fundamental oblique $\cos n_f \tilde{z} \cos \tilde{y}$ and the second oblique subharmonic $\cos(n_f \tilde{z}/2) \cos 2\tilde{y}$. The latter modes thus spoil the perfect checkerboard pattern. The property of period-doubling however is very robust provided the forcing is sufficiently close to the neutral wavenumber. As the forcing wavenumber decreases from the neutral, the intensity of the interaction between the fundamental and the subharmonic decreases. These observations are in qualitative agreement with the experimental results of Liu *et al.* [40].

With one-frequency initial forcing at wavenumbers below the stability window, we observe evolution similar to the "synchronous instability" of experiments [40]. For the run shown in Fig. 10(a), the values generated by the parameters of the corresponding experiment were $\kappa = 0.18$ and $\lambda = 0.05$. One can see that oblique modes with $m = 2$ become important, and a *quasi-stationary* 3-D state develops when the noise level in the initial condition is low. The resulting film surface pattern shown in Fig. 10(b) looks similar to the one in Fig. 18 in [40]. Eventually, the patterns yield to chaos. We note that the appearance of synchronous patterns and their exact nature is dependent on the harmonic and noise content in the initial conditions. If the initial condition has a subharmonic component, i.e., $A_{sub} \neq 0$ in (12), the synchronous patterns appear in combination with period-doubling patterns. At even lower wavenumbers of the one-frequency forcing, the flow develops *solitary wave*-like transient patterns [see Fig. 11]. These patterns resemble to some degree the patterns in Fig. 2 of Ref. [40] obtained at low-frequency forcing (however, the experimental solitary waves seem to have large amplitudes and are likely to be strongly nonlinear).

Thus, the solutions of Eq. (8) qualitatively reproduce the experimentally observed types of transient patterns on inclined films, along with the correspondence of the pattern type to the forcing frequency.

4 Conclusion

By using the multiparametric perturbation approach, we have developed a theory of a wavy film flowing down an inclined plane. It includes an evolution PDE for film thickness and explicit expressions for pressure and velocities in terms of its solutions, as well as conditions of validity (both local-validity and global-validity ones). We argued that the PDE (4) for the film thickness is the most general equation derivable (from the full Navier-Stokes problem under consideration) as a rational, well-controlled approximation. For large-amplitude waves the approximation [and the Benney equation which is a particular

case of our equation (4)] cannot be good uniformly for all time. We pointed out however that Eq. (4) has a chance to avoid explosive solutions and thus can be preferable to the Benney equation as a qualitative model for the large-amplitude waves. In contrast, the small-amplitude evolution equation (8) *is* valid for all time provided the parametric conditions (7) are satisfied.

The numerical simulations of this equation in the case of large dispersion reveal unusual spatiotemporal patterns on the system attractors. These nonstationary 3-D patterns are highly organized but differ from other patterns which have been usually studied in nonequilibrium dissipative systems: the new patterns are not simply periodic, even locally. The patterns we have found consist of two subpatterns which percolate through each other (each subpattern by itself is almost stationary; one of them is essentially nonperiodic, but both are highly ordered). Experiments which would satisfy the conditions of validity of our theory require highly viscous liquids, such as glycerol and its water solutions.

For the parameters of the recent experiments [40], preliminary results of our simulations are in qualitative agreement with the 3-D transient patterns observed in those experiments: subharmonic interactions and checkerboard patterns at near-neutral frequencies of forcing, synchronous (i.e. with no period-doubling) transverse deformations of waves at intermediate frequencies, and solitary waves at low frequencies. This is despite the fact that the experimental parameters are somewhat outside the domain of guaranteed validity of our theory. We have also observed the formation of stationary waves for a certain range of forcing frequencies which has been also obtained theoretically.

While the validity of the evolution equation is obviously more limited than that of less drastic simplifications of the full Navier-Stokes problem, evolution equations have the advantage of being much more amenable to numerical simulations and theoretical studies. Results obtained for small-amplitude equations—derived as well-controlled approximations with known conditions of validity—might lead to insights useful for the studies of even large-amplitude waves on flowing films.

We are grateful to Mr. I. Yakushin, Dr. A. Minga, and Mr. X. Zhang for technical assistance. We have used the computing facilities of the Alabama Supercomputer Authority and the National Energy Research Supercomputing Center of the Department of Energy.

A The full NS problem

In a coordinate system moving with a velocity V in the z-direction, the Navier-Stokes (NS) equations in the dimensionless form are (see e.g. [2])

$$u_t + uu_x + vu_y + wu_z - Vu_z = -p_x - 2\cot\theta/R + (u_{xx} + u_{yy} + u_{zz})/R, \tag{14}$$

$$v_t + uv_x + vv_y + wv_z - Vv_z = -p_y + (v_{xx} + v_{yy} + v_{zz})/R, \tag{15}$$

$$w_t + uw_x + vw_y + ww_z - Vw_z = -p_z + 2/R + (w_{xx} + w_{yy} + w_{zz})/R. \tag{16}$$

The continuity equation is

$$u_x + v_y + w_z = 0. \tag{17}$$

The boundary conditions are as follows. The no-slip conditions at the surface are

$$u = v = w = 0 \quad \text{at} \quad x = 0. \tag{18}$$

The tangential-stress balance conditions at the free surface are

$$p_{11}h_y + p_{12}[1 - {h_y}^2] - p_{13}h_yh_z - p_{22}h_y - p_{23}h_z = 0, \tag{19}$$

$$p_{11}h_z + p_{13}[1 - {h_z}^2] - p_{12}h_y h_z - p_{23}h_y - p_{33}h_z = 0. \tag{20}$$

The normal-stress balance condition is

$$[p_{11} + p_{22}{h_y}^2 + p_{33}{h_z}^2 - 2p_{12}h_y + 2p_{23}h_y h_z - 2p_{13}h_z][1 + {h_y}^2 + {h_z}^2]^{1/2} = \gamma[h_{yy}\{1 + {h_z}^2\} + h_{zz}\{1 + {h_y}^2\} - 2h_y h_z h_{zy}] \tag{21}$$

where the stress components are

$$\begin{aligned} p_{11} &= -p + 2u_x/R \qquad p_{12} = (u_y + v_x)/R, \\ p_{22} &= -p + 2v_y/R \qquad p_{23} = (v_z + w_y)/R, \\ p_{33} &= -p + 2w_z/R \qquad p_{13} = (u_z + w_x)/R. \end{aligned} \tag{22}$$

Finally, the kinematic condition at the free surface is

$$h_t + vh_y + wh_z - Vh_z = u. \tag{23}$$

B Expressions for velocity corrections

The expressions for the velocity components v, w_1, and u_1 in terms of h are

$$\begin{aligned} v &= -\frac{x^3}{3}h_{zy} - x^2\left[h_y h_z + hh_{zy} + W(\nabla^2 h)_y - \cot\theta h_y\right] \\ &\quad + x\left[8hh_y h_z + 4h^2 h_{zy} + 2hW(\nabla^2 h)_y - 2h\cot\theta h_y\right], \end{aligned} \tag{24}$$

$$\begin{aligned} w_1 &= \frac{x^4}{6}Rhh_z - \frac{x^3}{3}\left[\nabla^2 h + h_{zz} + 2Rh_z\right] \\ &\quad + x^2\left[-hh_{zz} + \cot\theta h_z - W(\nabla^2 h)_z - h_z h_z\right] \\ &\quad + x\left[h^2\nabla^2 h + 4h^2 h_{zz} - 2\cot\theta hh_z + 2Wh(\nabla^2 h)_z\right. \\ &\quad \left. + 2Rh^2 h_z - \frac{2}{3}Rh^4 h_z + 10hh_z h_z + 2hh_y h_y\right] \\ &\quad + \left(\frac{x^3}{3} - h^2 x\right)Rh_t, \end{aligned} \tag{25}$$

$$\begin{aligned} u_1 &= -\frac{x^5}{30}R(hh_z)_z + \frac{x^4}{6}\left[(\nabla^2 h)_z + Rhh_{zz}\right] \\ &\quad + \frac{x^3}{3}\left[\frac{1}{2}\nabla^2(h^2)_z - \cot\theta\nabla^2 h + W\nabla^4 h\right] \\ &\quad - \frac{x^2}{2}\left\{\left(h^2\nabla^2 h\right)_z + 4\left(h^2 h_{zz}\right)_z - 2\cot\theta\left[(hh_z)_z + (hh_y)_y\right]\right. \\ &\quad + 2W\left[\left(h\nabla^2 h_z\right)_z + \left(h\nabla^2 h_y\right)_y\right] + 2R\left(h^2 h_z\right)_z - \frac{2}{3}R\left(h^4 h_z\right)_z \\ &\quad \left. + 10\left(hh_z{}^2\right)_z + 2\left(hh_y{}^2\right)_z + 8\left(hh_y h_z\right)_y + 4\left(h^2 h_{zy}\right)_y\right\} \\ &\quad - \frac{x^4}{12}Rh_{tz} + \frac{x^2}{2}R(h^2 h_t)_z\ . \end{aligned} \tag{26}$$

References

[1] V. Y. Alekseenko, S. V. Nakoryakov and B. G. Pokusaev. Wave formation on a vertical falling liquid film. *AIChE J.*, 31:pp. 1446–1460, 1985.

[2] R. W. Atherton and G. M. Homsy. On the derivation of evolution equations for interfacial waves. *Chem. Engng Commun.*, 2:57–77, 1976.

[3] A. J. Babchin, A. L. Frenkel, B. G. Levich, and G. I. Sivashinsky. Nonlinear saturation of Rayleigh-Taylor instability. *Phys. Fluids*, 26:3159–3161, 1983.

[4] N. J. Balmforth, G. R. Ierely, and R. Worthing. Pulse dynamics in an unstable medium. Institute for Fusion Studies Report, IFSR#708, May 1995.

[5] A. M. Binnie. Experiments on the onset of wave formation on a film flowing down a vertical plane. *J. Fluid Mech.*, 2:551–553, 1957.

[6] H.-C. Chang. Wave evolution on a falling film. *Annu. Rev. Fluid Mech.*, 26:103–136, 1994.

[7] H.-C. Chang, M. Cheng, E. A. Demekhin, and D. I. Kopelevich. Secondary and tertiary excitation of three-dimensional patterns on a falling film. *J. Fluid Mech.*, 270:251–275, 1994.

[8] H.-C. Chang, E. A. Demekhin, and D. I. Kopelevich. Nonlinear evolution of waves on a vertically falling film. *J. Fluid Mech.*, 250:433–480, 1993.

[9] M. C. Cross and P. C. Hohenberg. Pattern formation outside of equilibrium. *Rev. Mod.Phys*, 65:851–1112, 1993.

[10] E. A. Demekhin, G. Y. Tokarev, and V. Y. Shkadov. Hierarchy of bifurcations of space-periodic structures in a nonlinear model of active dissipative media. *Physica D*, 52:338–361, 1991.

[11] C. Elphick, G. R. Ierley, O. Regev, and E. A. Spiegel. Interacing localized structures with Galilean invariance. *Phys. Rev. A*, 44:1110–1112, 1991.

[12] A. L. Frenkel. To be published.

[13] A. L. Frenkel. Nonlinear saturation of core-annular flow instabilities. In *Proc. Sixth Symp. on Energy Engineering Sciences, CONF-8805106 (Argonne National Laboratory, Argonne, Illinois)*, pages 100–107, 1988.

[14] A. L. Frenkel. On asymptotic multiparameter method: Nonlinear film rupture. In *Proc. Ninth Symp. on Energy Engineering Sciences, CONF-9105116, (Argonne National Laboratory, Argonne, Illinois)*, pages 185–192, 1991.

[15] A. L. Frenkel. Stability of an oscillating Kolmogorov flow. *Phys. Fluids A*, 3:1718–1729, 1991.

[16] A. L. Frenkel. Nonlinear theory of strongly undulating thin films flowing down a vertical cylinder. *Europhys. Lett.*, 18:583–588, 1992.

[17] A. L. Frenkel. On evolution equations for thin films flowing down solid surfaces. *Physics of Fluids A*, 5:2342–2347, 1993.

[18] A. L. Frenkel. Dissipative-dispersive evolution equation for falling annular films. *Bull. Am. Phys. Soc.*, 39:1856, 1994.

[19] A. L. Frenkel, A. J. Babchin, B. G. Levich, T. Shlang, and G. I. Sivashinsky. Annular flow can keep unstable flow from breakup: nonlinear saturation of capillary instability. *J. Colloid Interfac. Sci.*, 115:225–233, 1987.

[20] A. L. Frenkel and V. I. Kerchman. On large amplitude waves in core-annular flows. In *Proc. 14th IMACS Congress on Computations and Applied Mathematics*, volume 2, pages 397–400, Atlanta, 1994.

[21] A. L. Frenkel and G. Rudenko. Instabilities of space-time-periodic "triangular-eddy" flow. To be published.

[22] K. A. Gorshkov, L. A. Ostrovskii, and V. V. Papko. Interactions and bound states of solitons as classical particles. *Soviet Phys. JETP*, 44:306–311, 1976.

[23] T. Herbert. Secondary instabilities of boundary layers. *Annu. Rev. Fluid Mech.*, 20:487–526, 1988.

[24] K. Indireshkumar and A. L. Frenkel. To be published.

[25] S. W. Joo and S. H. Davis. Instabilities of three-dimensional viscous falling films. *J. Fluid Mech.*, 242:529–547, 1992; Irregular waves on viscous falling films. *Chem. Eng. Comm.*, 118:111–123, 1992.

[26] S. W. Joo, W. H. Davis, and S. G. Bankoff. On falling film instabilities and wave breaking. *Phys. Fluids*, 3:231–232, 1991.

[27] D. D. Joseph and Y. Renardy. *Fundamentals of Two-Fluid Dynamics*, volume II: Lubricated Transport, Drops, and Miscible Liquids. Springer, New York, 1993.
[28] D. D. Joseph and Y. Renardy. *Fundamentals of Two-Fluid Dynamics*, volume I: Mathematical Theory and Applications. Springer, New York, 1993.
[29] T. Kawahara. Formation of saturated solitons in a nonlinear dispersive system with instability and dissipation. *Phys. Rev. Lett.*, 51(5):381–383, 1983.
[30] T. Kawahara and S. Toh. Pulse interactions in an unstable dissipative-dispersive nonlinear system. *Phys. Fluids*, 31:2103–2111, 1988.
[31] R. E. Kelly. On the stability of an inviscid shear layer which is periodic in space and time. *J. Fluid Mech.*, 27:657–689, 1967.
[32] V. I. Kerchman and A. L. Frenkel. Interactions of coherent structures in a film flow: Simulations of a highly nonlinear evolution equation. *Theoret. Comput. Fluid Dynamics*, 6:235–254, 1994.
[33] W. B. Krantz and S. L. Goren. Finite-amplitude, long waves on liquid films flowing down a plane. *Ind. Engng Chem. Fundam.*, 9:107–113, 1970.
[34] M. V. G. Krishna and S. P. Lin. Nonlinear stability of a viscous film with respect to three-dimensional side-band disturbances. *Phys. Fluids*, 20:1039–1044, 1977.
[35] Y. Kuramoto and T. Tsuzuki. Persistent propagation of concentration waves in disspative media far from thermal equilibrium. *Progr. Theor. Phys.*, 55:356–369, 1976.
[36] E. M. Lifshitz and L. P. Pitaevsky. *Statistical Physics*, Part 2: Theory of Condensed Matter (in Russian; vol. 9 of Landau and Lifshitz's Theoretical Physics). Nauka, Moscow, 1978.
[37] S. P. Lin and C. Y. Wang. Modeling wavy film flows. In *Encyclopedia of Fluid Mechanics* (ed. N. P. Cheremisinoff), vol. 1, pp. 931-951. Gulf, Houston, 1985.
[38] J. Liu and J. P. Gollub. Solitary wave dynamics of film flows. *Phys. Fluids*, 6:1702–1712, 1994.
[39] J. Liu, J. D. Paul, and J. P. Gollub. Measurments of the primary instabilities of film flows. *J. Fluid Mech.*, 220:69–101, 1993.
[40] J. Liu, J. B. Schneider, and J. P. Golub. Three dimensional instabilities of flowing films. *Phys. Fluids.*, 7:55–67, 1995.
[41] C. Nakaya. Long waves on a thin fluid layer flowing down an inclined plane. *Phys. Fluids*, 18:1407–1420, 1975.
[42] A. A. Nepomnyashchy. Three-dimensional spatially-periodic motions in liquid films flowing down a vertical plane. *Hydrodynamics (Russian) Perm*, 7:43–52, 1974.
[43] A. Pumir, P. Manneville, and Y. Pomeau. On solitary waves running down an inclined plane. *J. Fluid Mech.*, 135:27–50, 1983.
[44] P. Rosenau, A. Oron, and J. M. Hyman. Bounded and unbounded patterns of the Benney equation. *Phys. Fluids A*, 4:1102–1104, 1992.
[45] G. J. Roskes. Three dimensional long waves on a liquid film. *Phys. Fluids*, 13:1440–1445, 1970.
[46] G. Sivashinsky. Nonlinear analysis of hydrodynamic instability in laminar flames. *Acta Astronaut.*, 4:1175–1206, 1977.
[47] G. Sivashinsky and A. Frenkel. On negative eddy viscosity under conditions of isotropy. *Phys. Fluids A*, 4:1608–1610, 1992.
[48] S. Toh, H. Iwasaki, and T. Kawahara. Two-dimensionally localized pulses of a nonlinear equation with dissipation and dispersion. *Phys. Rev. A*, 40:5472–5475, 1989.
[49] J. Topper and T. Kawahara. Approximate equations for long nonlinear waves on a viscous film. *J. Phys. Soc. Japan*, 44(2):663–666, 1978.
[50] Y. Y. Trifonov and O. Y. Tsvelodub. Nonlinear waves on the surface of a falling liquid film part i. *J. Fluid Mech.*, 229:531–554, 1991.
[51] N. J. Zabusky and M. D. Kruskal. Interaction of solitons in a collisionless plasma and the recurrence of initial states. *Phys. Rev. Lett.*, 15:240–243, 1965.